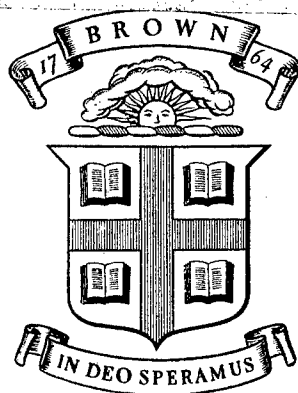


BZL  
ARPA-E-38

AD 65132



Division of Engineering  
BROWN UNIVERSITY  
PROVIDENCE, R. I.

STRESS-GRAIN SIZE ANALYSIS OF THE  
BRITTLE FRACTURE TRANSITION OF STEEL

R. W. ARMSTRONG

AD651322

ROUTED IN

Advanced Research Projects Agency  
and Oak Ridge Associated Universities

ARPA E38

February 1967

TECHNICAL LIBRARY  
BLDG 313  
ABEEDEN PROVING GROUND, MD.  
STRAP-TL

ARPA-E-38

# Stress-Grain Size Analysis of the Brittle Fracture Transition of Steel\*

R. W. Armstrong

Brown University

Providence, Rhode Island

## Abstract

The temperature interval in which steel may show a fairly abrupt change from ductile to brittle behavior has been quantitatively specified in terms of the (Hall-Petch) stress-grain size parameters already reported in the literature from tests at various temperatures and strain rates. The transition in behavior depends in an important way on each one of all the stress components normally combined in a single yield stress or fracture stress measurement.

---

\* This study was supported at Brown University by the Advanced Research Projects Agency and at the Solid State Division of the Oak Ridge National Laboratory through a Summer (1966) Research Participant Appointment by the Oak Ridge Associated Universities.

20060223360

TECHNICAL LIBRARY  
BLDG. 813  
ABERDEEN PROVING GROUND, MD.  
STEAP-TL

# Stress-Grain Size Analysis of the Brittle Fracture Transition of Steel

## 1. Introduction

For steel, it has been shown experimentally that the brittle fracture stress,  $\sigma_c$ , and the ductile yield stress,  $\sigma_y$ , obey the following (Hall-Petch) stress-grain size relationships<sup>1-5</sup>,

$$\sigma_c = \sigma_{o_c} + k_c \ell^{-1/2} \quad (1a)$$

$$\sigma_y = \sigma_{o_y}^* + B^1 \exp(-\beta^1 T) + k_y \ell^{-1/2} \quad (1b)$$

where  $\sigma_{o_c}$  is the stress intercept for brittle fracture at an extrapolated infinite grain size,  $k_c$  is the effective internal stress concentration associated with brittle fracture (the slope of  $\sigma_c$  plotted versus inverse square root of grain size),  $\ell$  is the average grain diameter,  $\sigma_{o_y}^*$  is the temperature independent contribution to the yield stress intercept,  $\beta^1$  is the exponential temperature coefficient of the temperature-sensitive part of the yield stress,  $B^1$  is the stress intercept of this yield component at 0°K,  $T$  is the absolute temperature and  $k_y$  is the stress concentration required at the tip of a slip band for initiating further plastic flow.

A previous analysis<sup>6</sup> also showed that a hypothetical ductile-brittle transition temperature,  $T_c$ , might be directly specified by equating  $\sigma_y$  and  $\sigma_c$  to obtain, from equations (1a) and (1b), the following expression:

$$T_c = \frac{1}{\beta^1} [\ln B^1 - \ln \{(k_c - k_y) + (\sigma_{o_c} - \sigma_{o_y}^*) \ell^{1/2}\} - \ln \ell^{-1/2}]. \quad (2)$$

The experimental situation has been extensively investigated by Hahn et al.<sup>7</sup> and is indicated in Figure 1. Here, the tensile yield stress is represented at high temperature by the solid curve which rises over a

substantial range of temperature as it decreases, until, at  $T_c$ , the yield stress intersects a fracture stress curve which is essentially independent of temperature. A complicating feature shown in Figure 1, and which will be discussed subsequently, is that, for large grain size specimens, at least, the ductile fracture stress curve, shown as the solid curve above the yield stress, may intersect this curve at a higher temperature,  $T_{dc}$ . Between  $T_c$  and  $T_{dc}$ , the yield stress and the tensile fracture stress are very nearly coincident. For small grain sizes, the ductile fracture stress is represented by the dashed curve originating at  $T_c$  and extending to higher temperatures. Below  $T_c$ , the yield stress continues to increase as the temperature decreases (the extrapolated dashed curve), as may be verified by testing in compression<sup>8</sup>.

The analysis leading to equation (2) has a similar basis to that proposed by Cottrell<sup>9</sup> and Petch<sup>10</sup> for the same phenomenon. Some differences do exist. The stress-grain size analysis gives a form of  $T_c$  which is completely determined without recourse to introducing the quantity specified by Cottrell and Petch as the effective surface energy of a cleavage crack. This is not to say that theory plays an unimportant role in the development and understanding of the equation given for  $T_c$ . Rather, the main theoretical considerations underlying this ductile-brittle transition temperature are only those which provide a basis for understanding the terms comprising the stress-grain size equations. For example, Stroh<sup>11</sup> has calculated the value of  $k_c$  from dislocation theory and the result for several metals, particularly, iron, is in agreement with experiment.

The purpose of the present investigation is to further elaborate on the features of specifying the ductile-brittle transition, principally, on the basis of equation (2).

## 2. The Yield Stress and the Fracture Stress

Table 1 contains some values of  $\sigma_c$ ,  $k_c$ ,  $\sigma_{oy}^*$ ,  $B^1$ ,  $\beta^1$  and  $k_y$  which apply for the several mild steel specimens listed as A, B, and A\*. The value of  $\sigma_c$  has been taken as a mean value determined from the data given by Petch<sup>2</sup> and by Low<sup>3</sup>. The value for  $k_c$  is taken from Petch<sup>2</sup> and the values of  $B^1$ ,  $\beta^1$  and  $k_y$  are due to Heslop and Petch<sup>4</sup>. The lower value of  $\sigma_{oy}^*$  has been estimated by Petch<sup>12</sup> as a typical value for well-annealed material, whereas the larger value corresponds to a stress level that might be produced by neutron irradiation damage<sup>13</sup>. Values of  $\sigma_{oy}^*$  less than this larger value could be produced by thermal quenching<sup>14</sup>.

The values of  $T_c$  corresponding to A, B, and A\* have been computed as shown in Figure 2. The results may be compared with those shown schematically in Figure 1. In Figure 2, the yield stress in compression equals the fracture stress in tension only for a small range in temperature centered on  $T_c$ , although this temperature range increases as  $T_c$  increases. As indicated in Table I, A and B are the same steel except for the difference in grain size. In this case, the transition is lower for the smaller grain size because of the inequality,  $k_c > k_y$ . A comparison of A and A\* shows the influence on  $T_c$  of  $\sigma_{oy}^*$ . The increase in  $T_c$  produced for A\* by an increase in  $\sigma_{oy}^*$  results because the brittle fracture parameters,  $\sigma_c$  and  $k_c$ , appear to be unchanged by variations in the distribution and amounts of solutes or precipitates.<sup>2</sup> In general,  $\sigma_c$  is taken to be relatively insensitive to composition, temperature, strain rate, and strain. This lack of influence is assumed to apply for neutron irradiation damage.

The strain rate,  $\dot{\epsilon}$ , should influence  $T_c$ . Petch<sup>12</sup> pointed out that this consideration enters equation (2) through the parameter,  $\beta^1$ ,

defined in (1b). An explicit dependence of  $\beta^1$  on  $\dot{\epsilon}$  has only recently been obtained<sup>15</sup> as a result of comparing the temperature dependent part of (1b) and the constitutive rate equation based on the thermally-activated motion of dislocations. In the aforementioned analysis the parameters  $B^1$  and  $\beta^1$  have the form

$$B^1 \approx 2 U_0 / v_0 \quad (3a)$$

and

$$\beta^1 = \beta_0^1 + \frac{R}{U_0} \ln \frac{\dot{\epsilon}_0^*}{\dot{\epsilon}}, \quad (3b)$$

where  $U_0$  is an activation energy for dislocation movement in the absence of external stress,  $R$  is Boltzmann's constant,  $v_0$  is the activation volume at  $0^\circ\text{K}$ , and  $\beta_0^1$  and  $\dot{\epsilon}_0^*$  are experimental constants. Theory and experiment reveal that  $\dot{\epsilon}_0^* > \dot{\epsilon}$  and, therefore, (3b) shows that  $\beta^1$  decreases as  $\dot{\epsilon}$  increases. The increase in  $T_c$  produced by an increase in  $\dot{\epsilon}$  may be calculated from (3b) and (2). Using the values;  $\beta_0^1 \approx 6.5 \times 10^{-3} \text{ } ^\circ\text{K}^{-1}$ ,  $U_0 \approx 8.8 \times 10^{-13} \text{ ergs}$ , and  $\dot{\epsilon}_0^* \approx 5 \times 10^8 \text{ sec}^{-1}$ , the results shown in Figure 3 are obtained. It may be seen that, for mild steel,

$$\frac{d \ln T_c}{d \ln \dot{\epsilon}} = \frac{1}{\frac{\beta_0^1 U_0}{R} + \ln \frac{\dot{\epsilon}_0^*}{\dot{\epsilon}}} \approx .015 \quad (4)$$

As will be described in the following discussion, the influence of  $\dot{\epsilon}$  on  $T_c$  is an important factor to be taken into account for a proper evaluation of the transition temperatures measured by the standard procedure of Charpy v-notch impact testing.

### 3. The Variation of $T_c$ with Grain Size and Type of Test

Strengthening a steel by refining its grain size is doubly important because, in addition to raising the values of  $\sigma_y$  and  $\sigma_c$ , the value of  $T_c$  is lowered.

Figure 4 shows the variation of  $T_c$  with  $\ell^{-1/2}$  for the steels listed in Table I. Curve (a) applies to the steel condition characterized in I by A and B. Curve (b) applies for steel in the condition typified by A\*. The explicit dependence of  $T_c$  on  $\ell^{-1/2}$  is obtained from equation (2) as

$$\frac{dT_c}{d\ell^{-1/2}} = -\frac{1}{\beta^1} \left[ \frac{1}{\ell^{-1/2} + \frac{\sigma_{oc} - \sigma_{oy}^*}{k_c - k_y}} \right] \quad (5)$$

According to the relative values of the various parameters in (5), the value of  $d T_c / d \ell^{-1/2}$  falls between the limits:

$$-\frac{1}{\beta^1 \ell^{-1/2}} \leq \frac{dT_c}{d\ell^{-1/2}} \leq -\frac{1}{\beta^1} \left[ \frac{k_c - k_y}{\sigma_{oc} - \sigma_{oy}^*} \right] \quad (6)$$

For tensile testing of material in varying conditions,  $d T_c / d \ell^{-1/2}$  is shown as function of  $\ell^{-1/2}$  as the solid curves of Figure 5. Curve (a) represents the lower limit of (6) using only the value of  $\beta^1$  given in Table I. Heslop and Petch<sup>16</sup> initially proposed that this type of dependence fitted the results they measured in Charpy tests, although a smaller value of  $\beta^1$  was reasoned to be operative because of the large effective strain rate occurring for impact testing. Curve (b) is the value of  $d T_c / d \ell^{-1/2}$  corresponding to (5) for steels of type A, B. Curve (c) is drawn to indicate the upper limit for (6) where the value of  $\beta^1$  is taken as  $10^{-2} \text{ } ^\circ\text{K}^{-1}$  and the factor in brackets is

taken as  $1.25 \times 10^{-2} \text{ cm}^{1/2}$ . These latter values might apply for several of the body-centered-cubic refractory metals.

The ductile-brittle transition temperature measured in a Charpy notch impact test differs from that measured in a tensile test for, at least, two reasons: (1), the effective strain rate is large compared to that encountered in conventional tensile testing, as mentioned earlier; and, (2), the inhomogeneous stress system requires consideration of a "plastic constraint factor"<sup>17</sup> to account for an increase in yield stress due to the localized deformation which is forced to occur at the specimen notch. The strain rate and the plastic constraint both contribute to an increased yield stress. Cottrell<sup>9</sup> has discussed this second consideration and he accounted for it in estimating  $T_c$  by raising  $\sigma_y$  by a constant factor. For the Charpy test, then, in the simplest approximation,  $\sigma_c$  may be equated to  $\alpha\sigma_y$ , so that

$$T_c = \frac{1}{\beta^1} [\ln(\alpha B) - \ln\{(k_c - \alpha k_y) + (\sigma_{oc} - \alpha\sigma_y^*)\ell^{1/2}\} - \ln \ell^{-1/2}] \quad (7)$$

and

$$\frac{dT_c}{d\ell^{-1/2}} \approx -\frac{1}{\beta^1} \left[ \frac{1}{\ell^{-1/2} + \frac{\sigma_{oc} - \alpha\sigma_y^*}{k_c - \alpha k_y}} \right] \quad (8)$$

where the value of  $\beta^1$  is appropriate to the effective strain rate.

The value of  $\alpha$  which is chosen is very important; Hill<sup>17</sup> predicted  $1 \leq \alpha \leq 2.6$  whereas Cottrell took  $\alpha = 3$ . For the present analysis, a value of  $\alpha = 2$  was chosen to give reasonable agreement between equations (7) and (8) and the respective experimental measurements. Thus, Meakin and Petch<sup>18</sup> determined  $d T_c / d \ell^{-1/2} \approx -3.1 \text{ } ^\circ\text{K cm}^{1/2}$  and, for  $\ell^{-1/2} = 17.4 \text{ cm}^{-1/2}$ ,  $T_c \approx 290 \text{ } ^\circ\text{K}$ . Taking  $\beta \approx 8.44 \times 10^{-3} \text{ } ^\circ\text{K}^{-1}$



for  $\dot{\epsilon} = 10^3 \text{ sec}^{-1}$  from (3b) and  $\alpha = 2$ , (8) gives  $d T_c / d \ell^{-1/2} = -2^\circ \text{K cm}^{1/2}$  and, for  $\ell^{-1/2} = 17.4 \text{ cm}^{-1/2}$ , (7) gives  $T_c \approx 260^\circ \text{K}$ . Curve (c) in Figure 4 and the dotted curve in Figure 5 represent the values of (7) and (8) calculated as a function of grain size.

A comparison of all the curves in these Figures indicates that  $d T_c / d \ell^{-1/2}$  is a less sensitive measure of the accuracy of such an analysis than the value of  $T_c$  itself.

#### 4. The Dependence of $T_c$ on $\sigma_{O_y}^*$

Strengthening a steel at room temperature by increasing  $\sigma_{O_y}^*$  and, hence,  $\sigma_y$  could be dangerous because of the unfavorable influence that  $\sigma_{O_y}^*$  has on (increasing)  $T_c$ . This influence is shown for steel A\* in Figure 2 and is observed again in the higher values of  $T_c$  associated with curve (b) over curve (a) in Figure 4.

The dependence of  $T_c$  on  $\sigma_{O_y}^*$  is greater as the grain size increases but this dependence is complex as may be shown by differentiating equation (7) with respect to  $\sigma_{O_y}^*$ , i.e.

$$\frac{d T_c}{d \sigma_{O_y}^*} = \frac{\alpha}{\beta^1} \left[ \frac{1 + \ell^{-1/2} \frac{d k_y}{d \sigma_{O_y}^*}}{(\sigma_{O_c} - \alpha \sigma_{O_y}^*) + (k_c - \alpha k_y) \ell^{-1/2}} \right] \quad (9)$$

For this situation, a term is included for a possible dependence of  $k_y$  on  $\sigma_{O_y}^*$  because neutron irradiation experiments have indicated, at least, for large values of  $\sigma_{O_y}^*$  that  $k_y$  may decrease as  $\sigma_{O_y}^*$  increases<sup>19</sup>.

For steels of type A and B, subjected to Charpy tests, with  $\ell^{-1/2} = 17.4 \text{ cm}^{-1/2}$  and  $d k_y / d \sigma_{oy}^* = 0$ ,  $d T_c / d \sigma_{oy}^* \approx 6.2 \times 10^{-8} \text{ } ^\circ\text{K cm}^2/\text{dyne}$ . This compares with values of  $2.9 \times 10^{-8} \text{ (} ^\circ\text{K/1000 psi) } ^\circ\text{K cm}^2/\text{dyne}$  given by Petch and  $3.5 \times 10^{-8} \text{ } ^\circ\text{K cm}^2/\text{dyne}$  given by Cottrell. However, the value of (9) is sensitive to the particular values of  $\ell^{-1/2}$ ,  $\sigma_{oy}^*$ , and  $d k_y / d \sigma_{oy}^*$  which are employed, as indicated in Figures 6 and 7. Curve (a) in Figure 6 applies for the calculation given above. Curve (b) applies for a value of  $\sigma_{oy}^* = 1.6 \times 10^9 \text{ dynes/cm}^2$ . Curve (c) applies for this same value of  $\sigma_{oy}^*$  and for  $d k_y / d \sigma_{oy}^* = -4.55 \times 10^{-2} \text{ cm}^{1/2}$ . In Figure 7, the value of (9) has been computed as a function of  $\sigma_{oy}^*$  for several values of  $\ell^{-1/2}$  and  $d k_y / d \sigma_{oy}^*$ . The value of  $\sigma_{oy}^*$  in the denominator of the term in brackets in (9) is taken as the initial value and so the real value of  $d T_c / d \sigma_{oy}^*$  is underestimated. Curve (a) applies for  $\ell^{-1/2} = 17.4 \text{ cm}^{-1/2}$  and  $d k_y / d \sigma_{oy}^* = 0$  while (c) corresponds to the same value of  $\ell^{-1/2}$  but with  $d k_y / d \sigma_{oy}^* = -4.55 \times 10^{-2} \text{ cm}^{1/2}$ . Curve (b) corresponds to  $\ell^{-1/2} = 30 \text{ cm}^{-1/2}$  with  $d k_y / d \sigma_{oy}^* = 0$  while (d) corresponds to (b) except that  $d k_y / d \sigma_{oy}^* = -4.55 \times 10^{-2} \text{ cm}^{1/2}$ .

The level of  $\sigma_c$  determines a practical limit to the amount that  $\sigma_{oy}^*$  may be increased. The very strong increase in  $d T_c / d \sigma_{oy}^*$  shown at certain values of  $\sigma_{oy}^*$  for curves (a)-(d) occurs when  $\sigma_{oy}^*$  approaches the limiting value of  $\sigma_c$ . However, it appears to be difficult to increase  $\sigma_{oy}^*$  by a large amount by conventional procedures. For example, Cracknell and Petch<sup>14</sup> managed to raise  $\sigma_{oy}^*$  to a level of  $\sim 10^9 \text{ dynes/cm}^2$  by resorting to quenching (EN2) mild steel from  $650^\circ\text{C}$  and ageing for one hour at  $150^\circ\text{C}$ .  $\sigma_{oy}^*$  may be increased to larger values by neutron irradiation. Hull and Mogford measured an increase in  $\sigma_{oy}^*$  of  $\sim 1.5 \times 10^9 \text{ dynes/cm}^2$  for an irradiation exposure of  $\sim 10^{20} \text{ neutrons/cm}^2$ .

The increase in  $T_c$  caused by an increase in  $\sigma_{oy}^*$  may be obtained from (7), by difference, as

$$\Delta T_c \approx -\frac{1}{\beta^1} \left[ \ln \left\{ 1 - \frac{\alpha \Delta \sigma_{oy}^*}{(\sigma_{oc} - \alpha \sigma_{oy}^*) + (k_c - \alpha k_y) \ell^{-1/2}} \right\} \right]. \quad (10)$$

(10) has been used in conjunction with the results of Hull and Mogford<sup>13</sup>, for  $\Delta \sigma_{oy}^*$  as a function of neutron irradiation flux,  $\phi$ , to calculate the dependence of  $\Delta T_c$  on  $\phi$ , as given for the points and dotted curve in Figure 8. For reason of simplicity, all other parameters in (10) were taken from Table I and an average value of  $\ell^{-1/2} \approx 17.4 \text{ cm}^{-1/2}$  was assumed. The results may be compared with the band for data presented by Pellini, Steele and Hawthorne for a variety of steels, as described by Wechsler<sup>20</sup>. A decrease in  $\ell^{-1/2}$  would shift the calculated points and dotted curve to the left. The agreement between the calculated points and the data seems reasonable enough to suggest that a part of the substantial variation in the data could be explained in terms of (10) if all of the appropriate parameters were known. Also, the value of  $\Delta(\ln \Delta T_c) / \Delta(\ln \phi)$  for the first two calculated points in Figure 8 is .48 and Wechsler has pointed out that Cottrell previously estimated that  $\Delta T_c$  should be proportional to  $\phi^{1/3}$ .

### 5. Ductile Cleavage

As shown schematically in Figure 1, essentially brittle fracture may occur for large grain size specimens in a temperature interval between  $T_c$  and a higher temperature, designated  $T_{dc}$ . At  $T_{dc}$  the ductile fracture stress equals the yield stress and, in the interval,  $T_{dc} - T_c$ , the fracture stress follows the temperature dependence of the yield stress.

A part of the reason for the observation that tensile fracture occurs at temperatures above  $T_c$  is undoubtedly due to the inherent experimental scatter and lack of predictability associated with the brittle fracture process. This is indicated in Table I and Figure 2 by the variation in stress level for  $\sigma_c$ . Hahn et al.<sup>7</sup> have observed that  $(T_{dc} - T_c)$  increases as  $\ell^{-1/2}$  decreases and this is in agreement with the trend shown in Figure 2.

An additional possibility exists that the experimental variation of  $(T_{dc} - T_c)$  with  $\ell^{-1/2}$  may be explained in terms of the dependence on grain size of the ductile fracture stress,  $\sigma_f$ . Petch<sup>21</sup> has shown experimentally that

$$\sigma_f = \sigma_{of} + k_f \ell^{-1/2} \quad (11)$$

and it is interesting to inquire about the relative values of  $\sigma_{of}$  and  $k_f$  that would be needed to explain the trend measured by Hahn et al. For the present consideration, (11) is assumed to apply for the true ductile fracture stress values taken at the varying strains occurring in specimens having different grain sizes. The influence of an increasing strain to fracture with decreasing grain size on the results of Petch is to suggest that the inequalities should hold:  $\sigma_{of} < \sigma_{oc}$  and  $k_f > k_c$ . Further, it may be seen by comparing  $\sigma_f$ ,  $\sigma_c$ , and  $\sigma_y$  versus  $\ell^{-1/2}$  that these inequalities must obtain for  $(T_{dc} - T_c)$  to increase with decrease in  $\ell^{-1/2}$ . Both inequalities are significant. The first one,  $\sigma_{of} < \sigma_{oc}$ , may be taken to imply that ductile cleavage requires a propagation stress for an existing cleavage crack because, in the limiting case,  $\sigma_{of}$  should be nearly zero. A reasonable interpretation of the second inequality is that for ductile cleavage, crack propagation

under conditions involving appreciable plastic work at the crack tip is the important fracture process to consider.

This interpretation of  $T_{dc}$  is consistent with the idea that  $T_c$  applies to the limiting situation where the initiation of one crack leads to brittle fracture while  $T_{dc}$  corresponds to the situation of numerous cracks being present but a stress is required for the propagation of any one of them. This reasoning is in agreement with the metallographic observations of Hahn et al<sup>7</sup> on the number of cracks observed in various specimens as a function of temperature and grain size. In addition, the results of Low<sup>3</sup> may be taken to indicate that near to  $T_c$ ,  $k_f > k_c$ . These several factors indicate that a change in fracture process as a function of  $\ell^{-1/2}$  and temperature should be involved, also, in a complete understanding of the experimental results.

## 6. Summary

A previous analysis showed that a hypothetical ductile-brittle transition temperature might be directly specified in terms of the (Hall-Petch) stress-grain size relationships,  $\sigma = \sigma_o + k\ell^{-1/2}$ , experimentally observed for both the ductile yielding and brittle fracture of steel. This temperature and its variation with grain size, strain rate and temperature-independent friction stress have now been numerically computed by utilizing the Petch parameters,  $\sigma_o$  and  $k$ , which are reported in the literature. The transition for tensile tests and also Charpy notch impact tests is considered.

The calculations indicate that the grain size dependence of the transition temperature is less sensitive to the material properties

and the type of test than is the transition temperature itself. The calculations bear out very well the idea that for a material susceptible to brittle fracture a large grain size is to be avoided. In this connection, the following points are emphasized: (1) the transition temperature increases at an increasing rate with increase in  $\sigma_{oy}^*$ ; and, (2) the increase in transition temperature produced by adding to  $\sigma_{oy}^*$  is larger the larger the grain size of the material. These two points seem especially important because the principal influence of neutron irradiation damage for b.c.c. metals appears to be reflected in an increase of  $\sigma_{oy}^*$ . Limiting values also seem to result from the analysis for the maximum increase in  $\sigma_{oy}^*$  that may be accomplished by neutron irradiation.

The analysis involves some theoretical interpretation of the components measured in the stress-grain size relationship as well as involving an extension of the development towards understanding the nature of ductile cleavage. The analysis gives support to the view that  $T_c$  corresponds to the stress required for nucleation of a single unstable crack. For material with a large grain diameter, at least, propagation of one of a number of cracks may cause brittle fracture at higher temperatures than  $T_c$ .

7. References

1. E. O. Hall: Proc. Phys. Soc. London, 1951, vol. B64, p. 747.
2. N. J. Petch: J. Iron Steel Inst., 1953, vol. 174, p. 25.
3. J. R. Low: "Relation of Properties to Microstructure", ASM, Cleveland, 1953, p. 163.
4. J. Heslop and N. J. Petch: Phil. Mag., 1956, vol. 1, p. 866.
5. R. W. Armstrong, I. Codd, R. M. Douthwaite and N. J. Petch: Phil. Mag., 1962, vol. 7, p. 45.
6. R. W. Armstrong: Phil. Mag., 1964, vol. 9, p. 1063.
7. G. T. Hahn, B. L. Averbach, W. S. Owen and M. Cohen: "Fracture", Technology Press and John Wiley, New York, 1959, p. 91.
8. G. A. Alers, R. W. Armstrong and J. H. Bechtold: Trans. Met. Soc. AIME, 1958, vol. 212, p. 523.
9. A. H. Cottrell: ibid, p. 192.
10. N. J. Petch: Phil. Mag., 1958, vol. 3, p. 1089.
11. A. N. Stroh: Advanc. Phys., 1957, vol. 6, p. 418.
12. N. J. Petch: "Fracture", Technology Press and John Wiley, New York, 1959, p. 54.
13. D. Hull and I. L. Mogford: Phil. Mag., 1958, vol. 3, p. 1213.
14. A. Cracknell and N. J. Petch: Acta Met., 1955, vol. 3, p. 186.
15. R. W. Armstrong: Acta Met., 1967, in press.
16. J. Heslop and N. J. Petch: Phil. Mag., 1958, vol. 3, p. 1128.
17. R. Hill: "Plasticity", Clarendon Press, Oxford, 1950, p. 245.
18. J. D. Meakin and N. J. Petch: "Fracture of Solids", Interscience, New York, 1963, p. 393.
19. J. D. Campbell and J. Harding: "Response of Metals to High Velocity Deformation", Interscience, New York, 1961, p. 51.

20. M. S. Wechsler: "The Interaction of Radiation with Solids",  
North Holland, Netherlands, 1964, p. 296.
21. N. J. Petch: Phil. Mag., 1956, vol. 1, p. 866.



Table and Figures

Table I: Stress-grain size parameters for mild steel.

Figure 1: Schematic temperature variation of yield stress, brittle fracture stress and ductile fracture stress.

Figure 2: Calculated yield and fracture stresses for mild steel as a function of temperature.

Figure 3: The variation of  $d \log T_c / d \log \dot{\epsilon}$  with  $\dot{\epsilon}$ .

Figure 4: The dependence of  $T_c$  on  $\ell^{-1, 2}$  for two steel conditions and two types of test.

Figure 5: The dependence of  $d T_c / d \ell^{-1/2}$  on  $\ell^{-1/2}$  for several steel conditions and two types of test.

Figure 6: The dependence of  $d T_c / d \sigma_{oy}^*$  on  $\ell^{-1/2}$  for several steel conditions by Charpy notch impact tests.

Figure 7: The dependence of  $d T_c / d \sigma_{oy}^*$  on  $\sigma_{oy}^*$  for several grain sizes and steel conditions by Charpy notch impact tests.

Figure 8: The dependence of  $T_c$  on neutron flux,  $\phi$ .

TABLE OF STRESS-GRAIN SIZE PARAMETERS FOR MILD STEEL

STEEL	$\beta'$ , $^{\circ}\text{K}^{-1}$	$B'$ $10^8 \frac{\text{dynes}}{\text{cm}^2}$	$k_c$ $10^7 \frac{\text{dynes}}{\text{cm}^{3/2}}$	$k_y$ $10^7 \frac{\text{dynes}}{\text{cm}^{3/2}}$	$\sigma_{oc}$ $10^8 \frac{\text{dynes}}{\text{cm}^2}$	$\sigma_{oy}^*$ $10^8 \frac{\text{dynes}}{\text{cm}^2}$	$d^{-\frac{1}{2}},$ $-\frac{1}{2}$ $\text{cm}$
A	.0143	178	$21 \pm 1$	$7.3 \pm 0.1$	$33 \pm 5$	3	10
B	"	"	"	"	"	"	44.6
A*	"	"	"	"	"	29	10

TABLE I

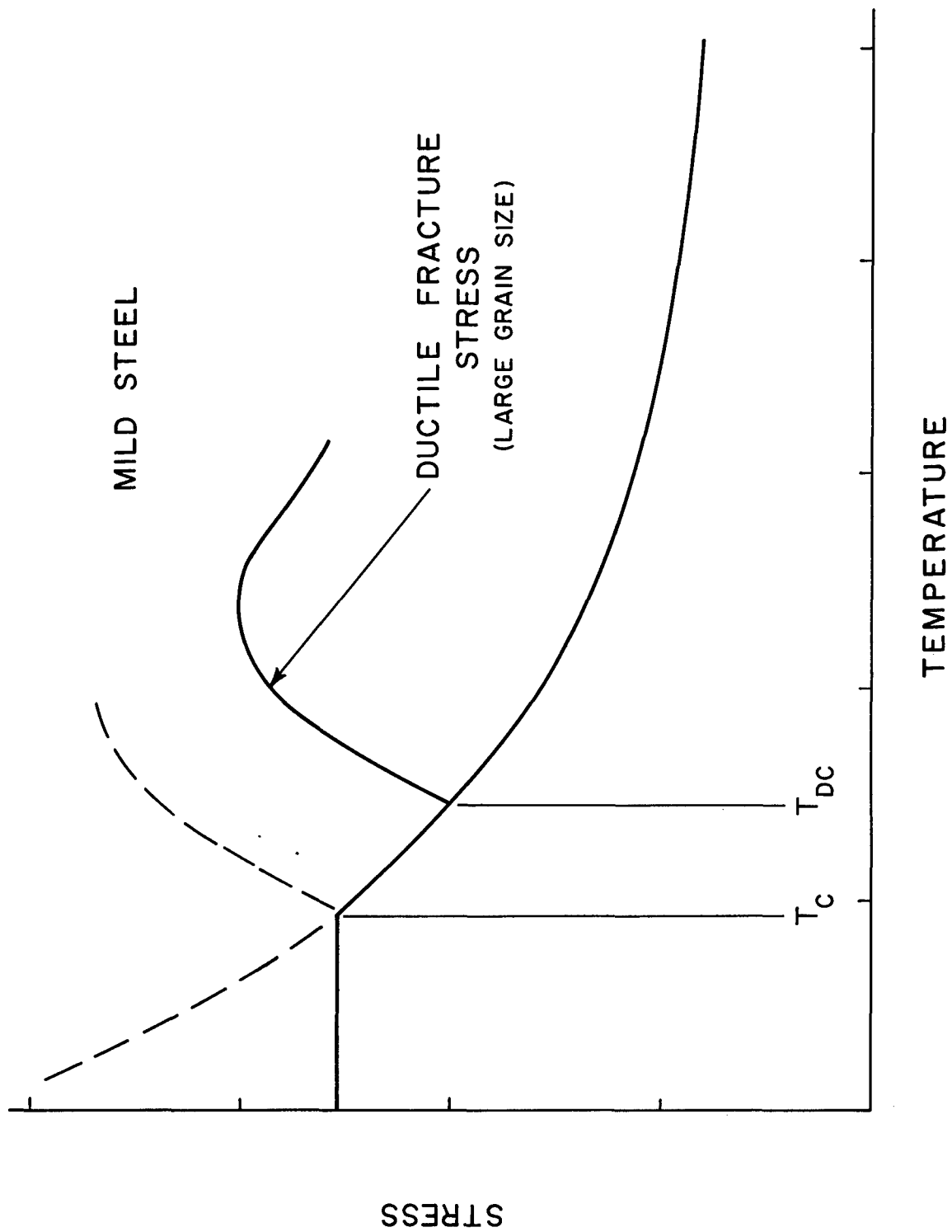


FIGURE I

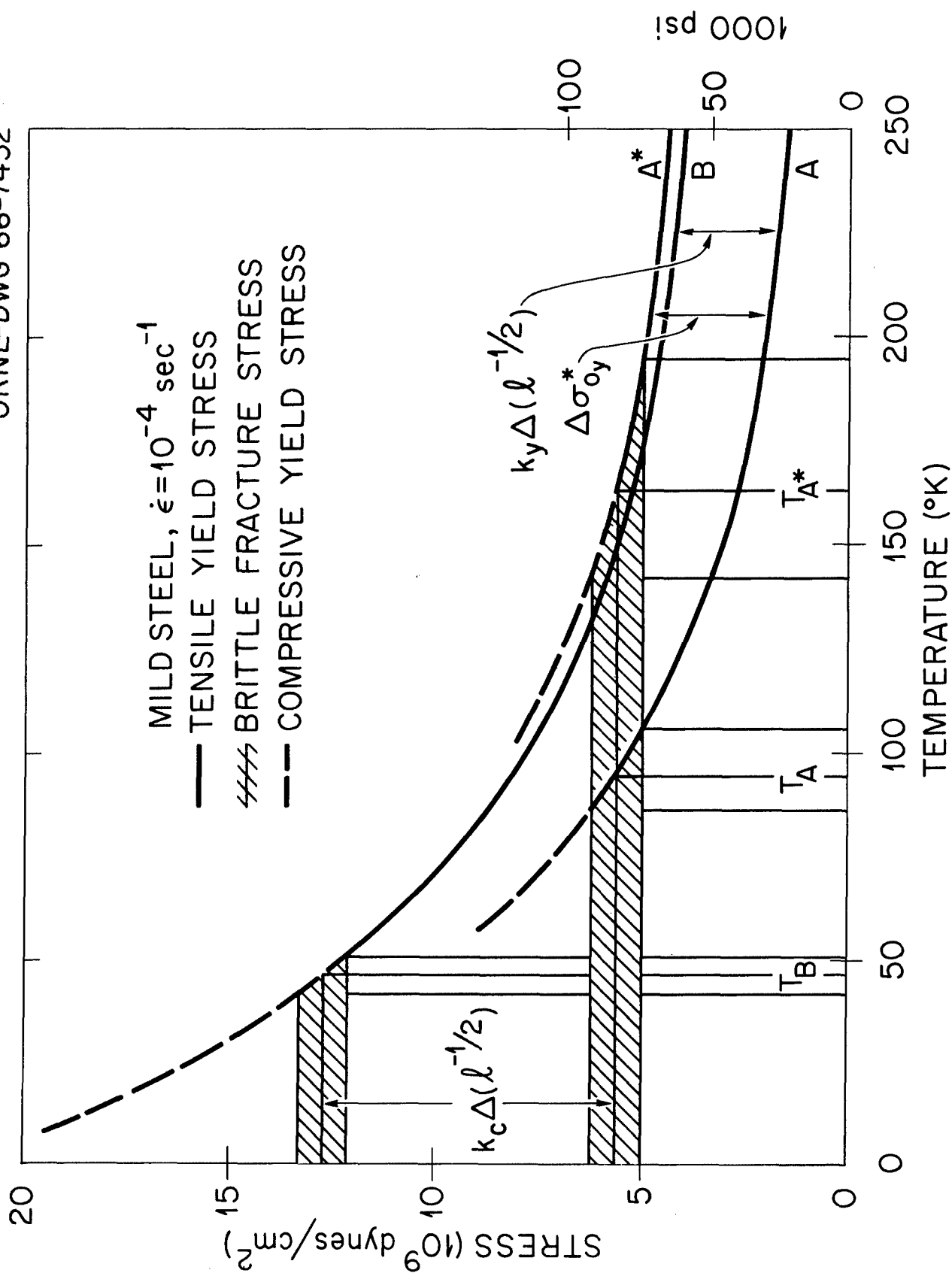


FIGURE 2

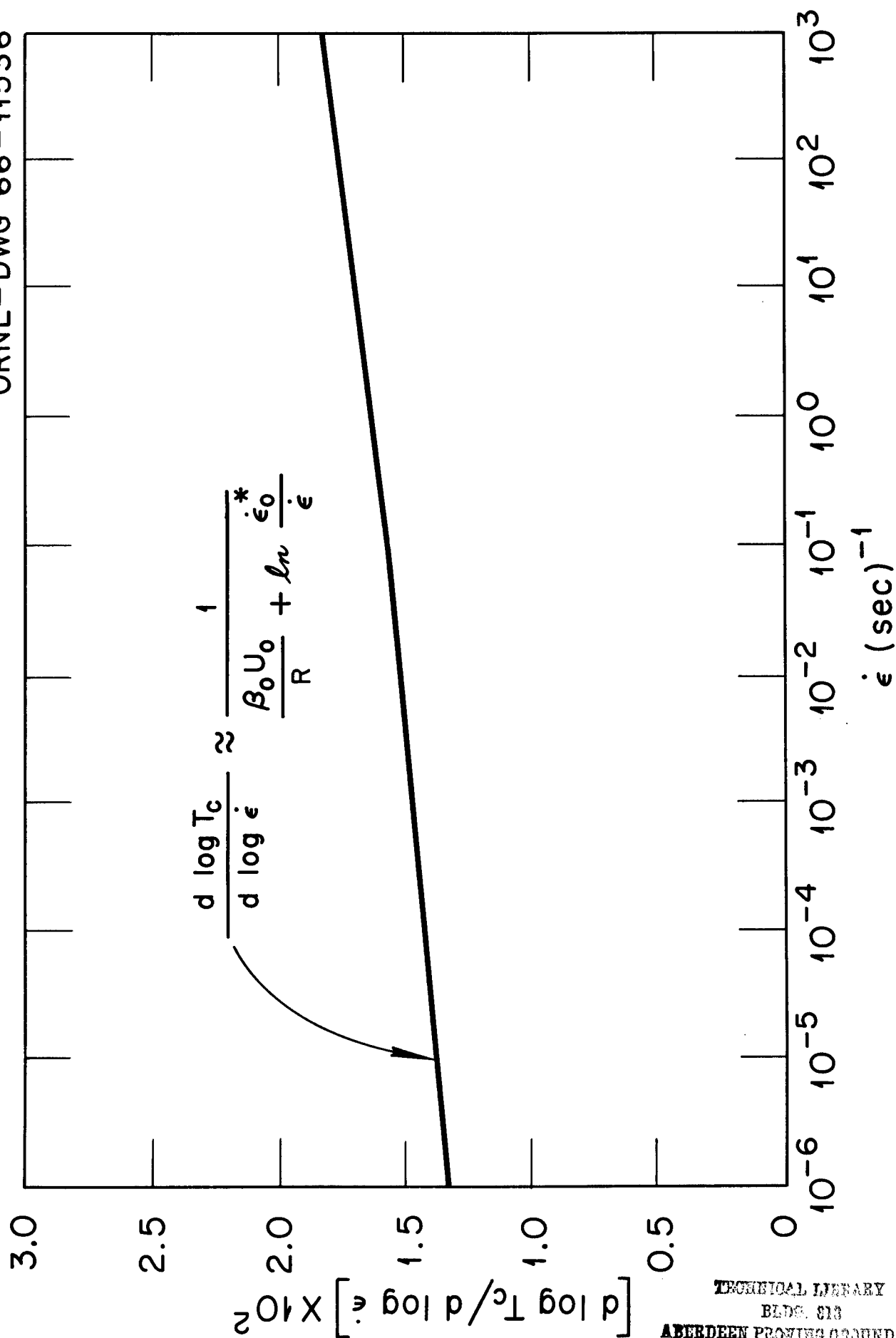


FIGURE 3

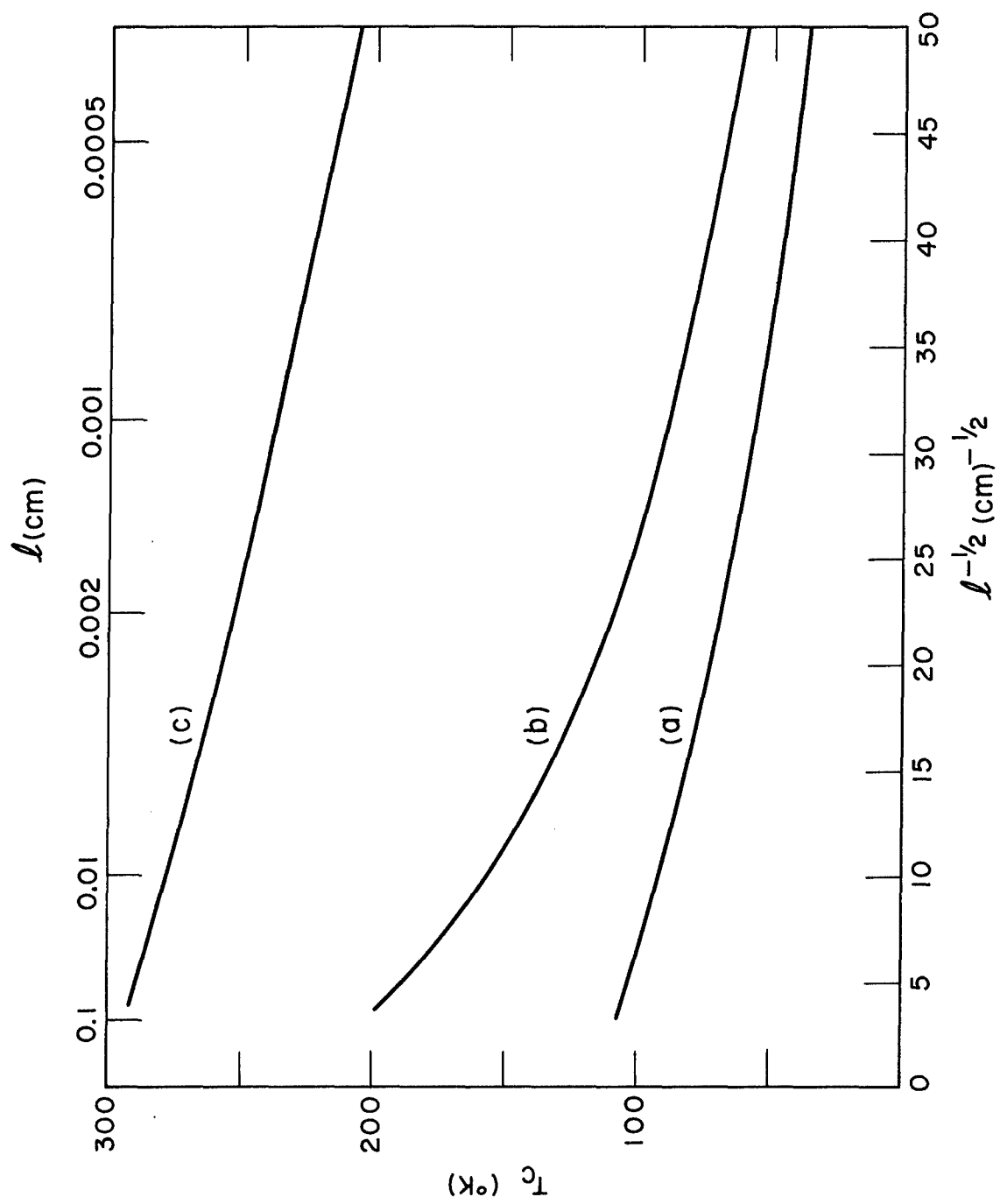


FIGURE 4

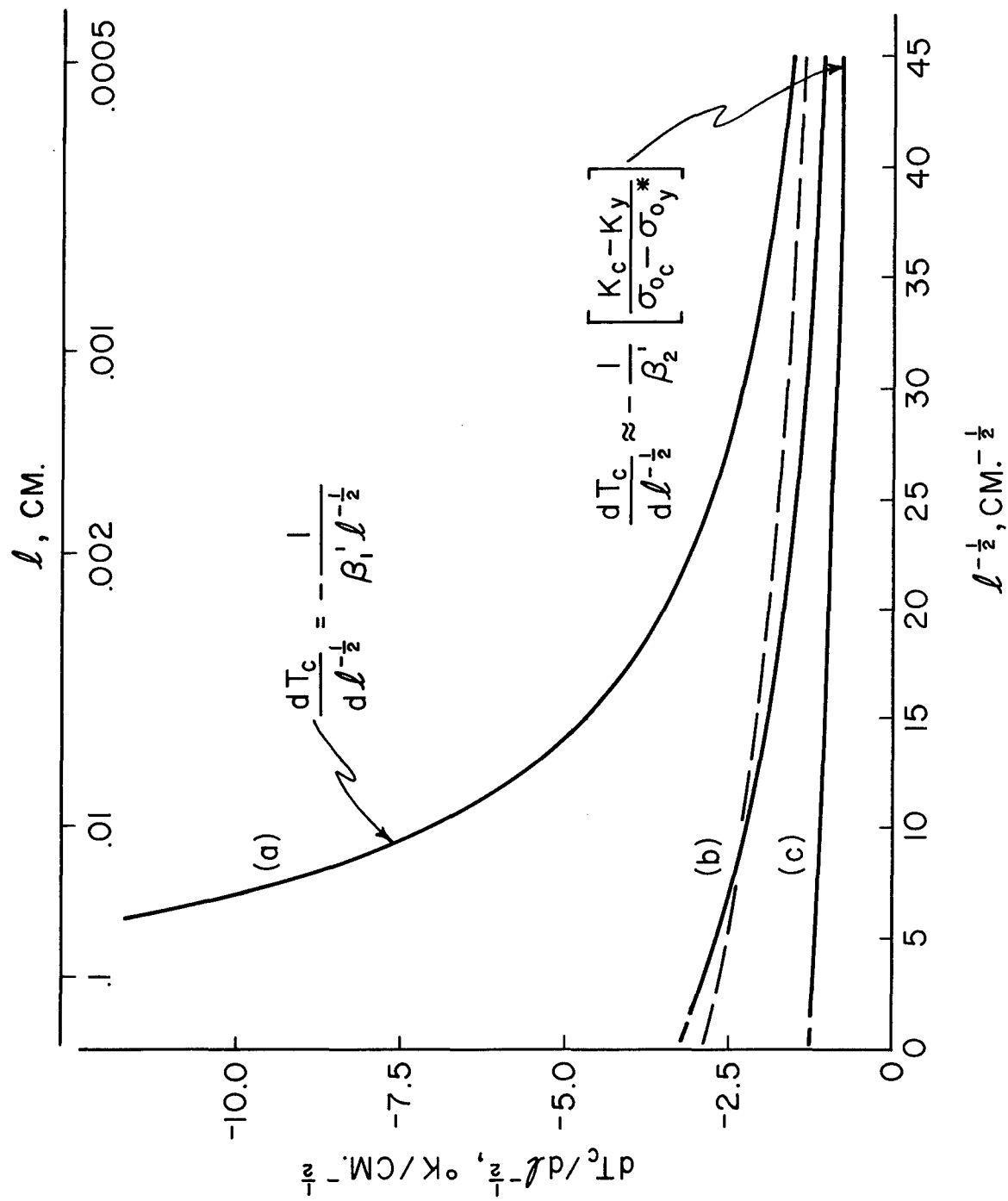


FIGURE 5

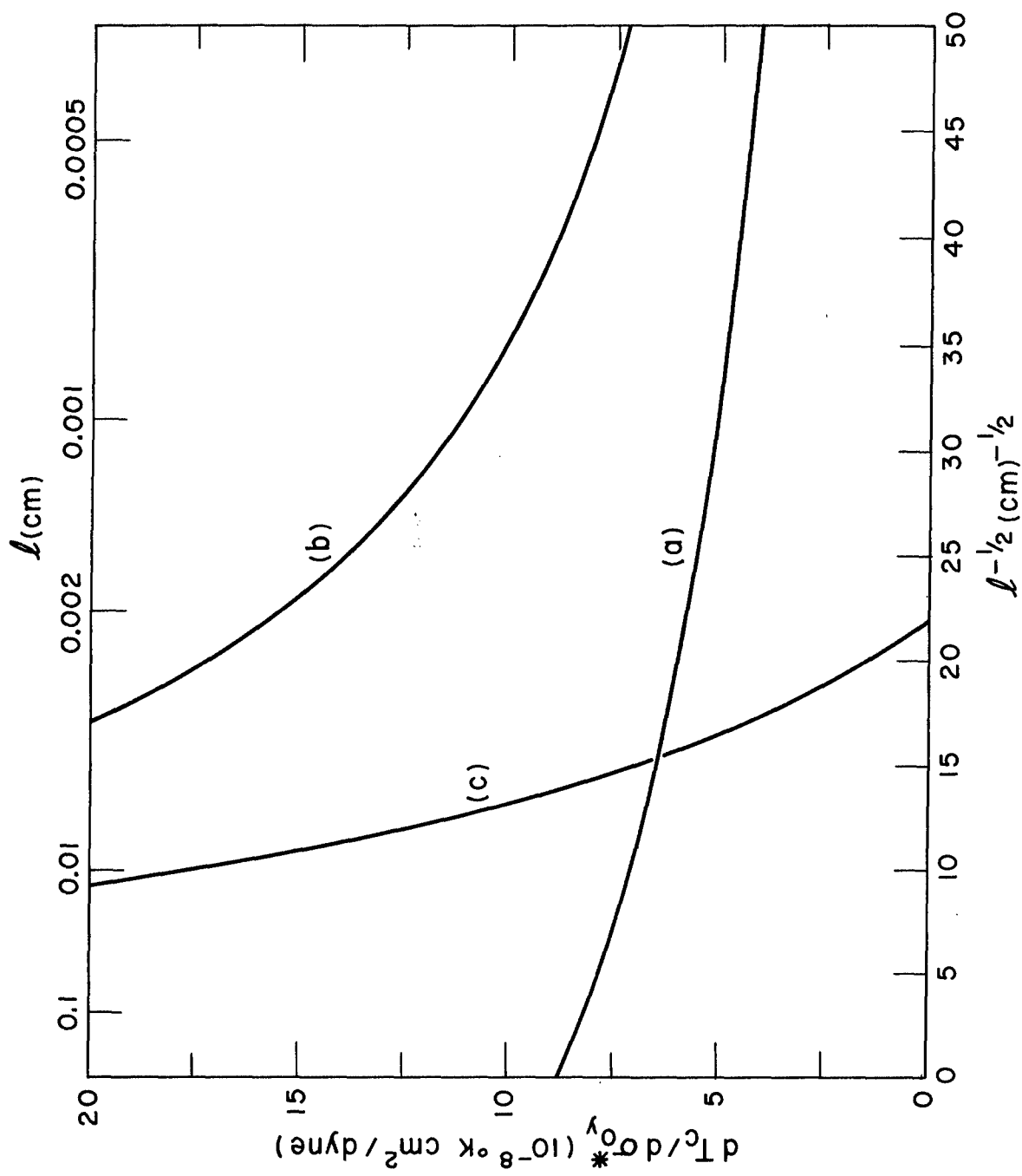


FIGURE 6



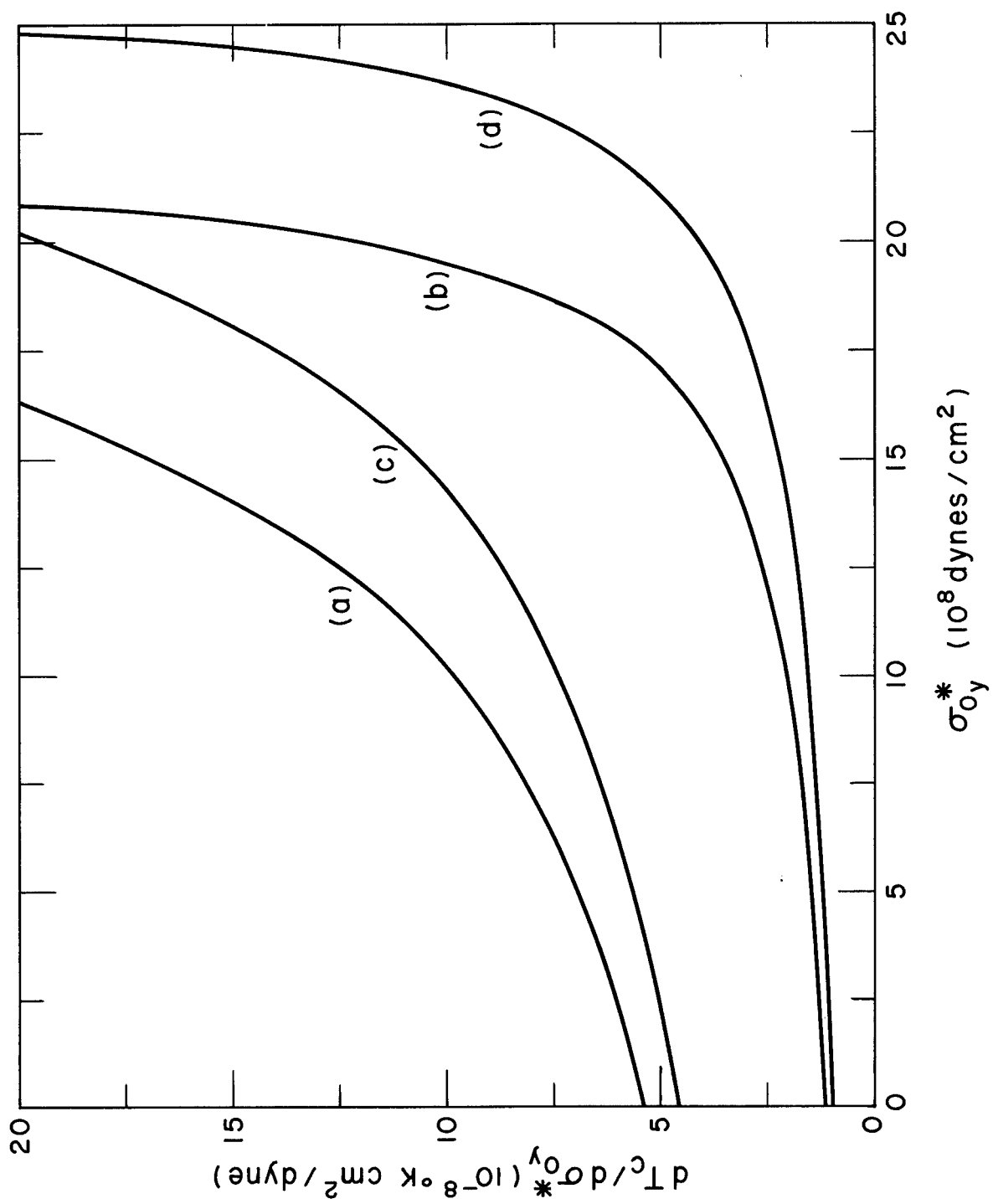


FIGURE 7

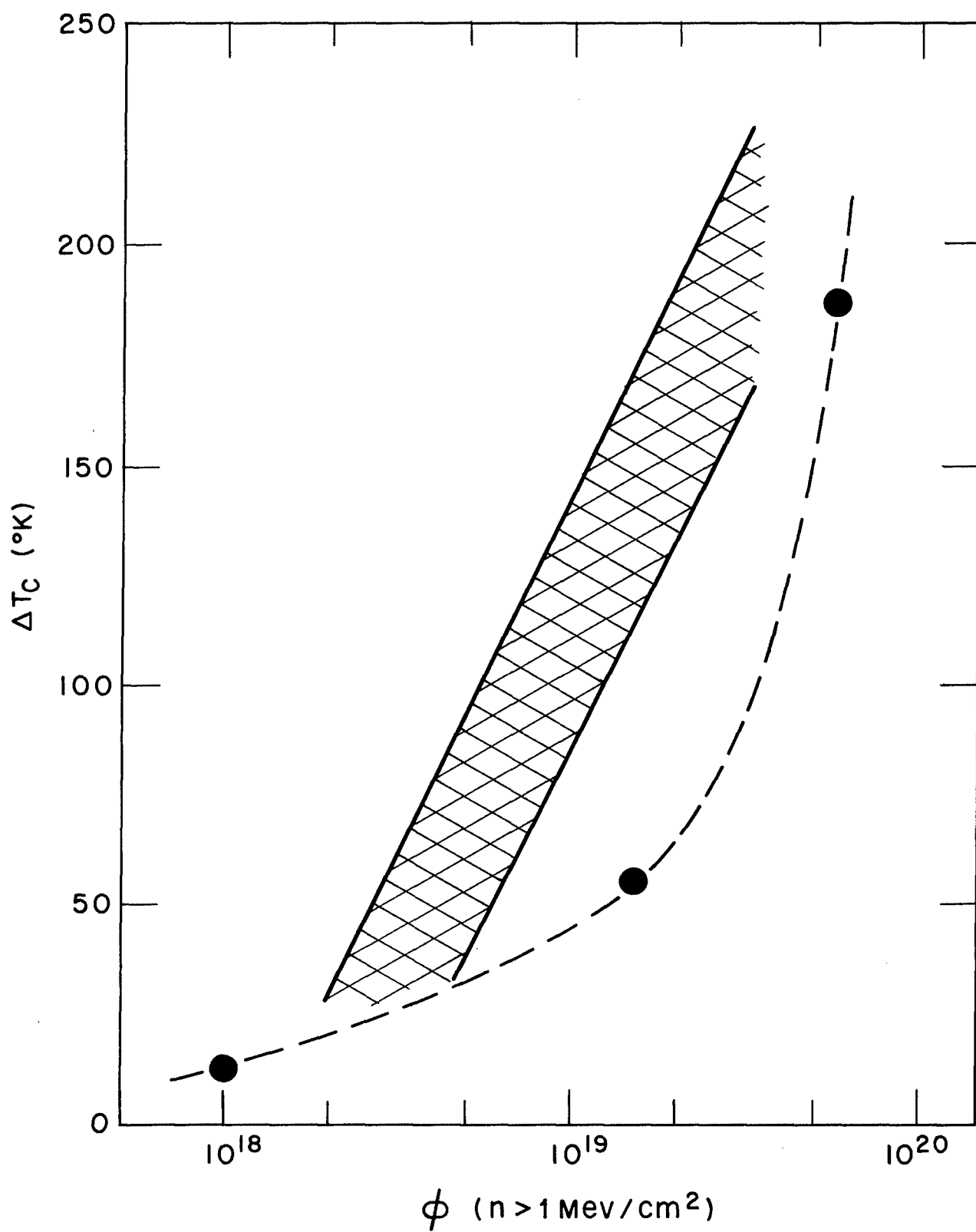


FIGURE 8